Applied Surface Science 324 (2015) 710–717

Contents lists available at ScienceDirect

Applied Surface Science

journal homepage: www.elsevier.com/locate/apsusc

Formation of Ag nanowires on graphite stepped surfaces. A DFT study

Rubén E. Ambrusi [a], Silvana G. García [a], María E. Pronsato [b,*]

[a] Departamento de Ingeniería Química, Universidad Nacional del Sur e Instituto de Ing. Electroquímica y Corrosión (INIEC), Av. Alem 1253, 8000 Bahía Blanca, Argentina
[b] Departamento de Física, Universidad Nacional del Sur & IFISUR (UNS – CONICET), Av. Alem 1253, 8000 Bahía Blanca, Argentina

ARTICLE INFO

Article history:
Received 9 June 2014
Received in revised form 1 October 2014
Accepted 5 November 2014
Available online 13 November 2014

Keywords:
Adatoms
Atom–solid interaction
Surface energy
Graphite
Silver
Density functional calculations

ABSTRACT

We investigate the feasibility of obtaining silver nanowires on graphite stepped surfaces theoretically, using density functional theory calculations. Three layer slabs are used to model graphite surfaces with and without defects. Adsorption energies for Ag atoms on graphite surfaces were calculated showing the preference of Ag adatoms to locate on the steps, forming linear structures like nanowires. An analysis of the charge densities and projected densities of states for different structures is also performed.

1. Introduction

The development of metallic nanowires has attracted much attention in recent years because of the interesting chemical, physical and mechanical properties that present these structures as well as for their potential applications in nanotechnology. Different methods have been employed to obtain nanowires [1]. One of them is electrochemical deposition in which the metal of interest can be electrodeposited into porous masks or the nanowire can be obtained by preferential deposition at the step edges of the highly oriented pyrolytic graphite (HOPG) [2]. In particular, Ag nanowires can be used as electrosensors for amines [3], or as the basis for more sophisticated nanostructures synthesis with other applications. There are extensive experimental results of the Ag-graphite system [4–9] as well as theoretical studies of Ag adsorption on graphite surfaces without defects [10–16]. These results are, at the same time, supported by scanning tunneling microscopy (STM) characterization of graphite substrates after Ag evaporation on this surface [17,18].

In this work, we employ density functional theory (DFT) calculations to evaluate the interaction between Ag atoms and (0 0 0 1) graphite surfaces without defects and with a step in the [0 1 0 0] direction. The latter system is similar to that found in Ag electrochemical deposits on HOPG, wherein the substrate is a surface composed of flat terraces and regions with steps. In a first stage, DFT parameters, such as cut off energy, *k*-point set, smearing function; were optimized for bulk graphite, by calculating known properties for the ground state and comparing the results with experimental data in the literature. Then, slab models were built for the surface with and without defects. For both types of surfaces, adsorption of Ag atoms was studied determining the most favorable sites for adsorption. Adsorption energies for systems with different geometrical configurations for the stepped surface were also evaluated in order to examine the feasibility of developing aligned structures such as nanowires on graphite stepped edges.

2. Computational method

DFT with calculations with Van der Waals corrections were performed using the Viena Ab-initio Simulation Package (VASP) [19–22], which employs a plane-wave basis set and a periodic supercell method. The generalized gradient corrected approximation (GGA) functional Perdew, Burke, and Ernzerhof (PBE) was used [23]. The Kohn–Sham equations were solved variationally using the projector-augmented-wave (PAW) method [24,25]. For the Van der Waals description, we adopt Grimme's DFT-D2 approach [26]. In order to test the validity of the method employed, some additional calculations were performed using the vdw-DF2 method to account for the Van der Waals forces [27] and the results compared with

* Corresponding author. Tel.: +54 291 4595142; fax: +54 291 4595142.
E-mail address: pronsato@criba.edu.ar (M.E. Pronsato).

http://dx.doi.org/10.1016/j.apsusc.2014.11.023
0169-4332/

Table 1
Surface energy calculation as a function of the number of layers, and dispersion energy of the slab (E_{vdw}).

Number of layers	Surface energy (J/m^2)	E_{vdw} (eV)
1	0.18	−0.11
2	0.18	−0.35
3	0.19	−0.59
4	0.19	−0.84
5	0.19	−1.09
6	0.19	−1.33
7	0.19	−1.58
8	0.19	−1.83
9	0.19	−2.08
10	0.19	−2.33
11	0.19	−2.57
12	0.19	−2.82
13	0.19	−3.07
14	0.19	−3.32

those previously obtained. Spin polarization was considered in all calculations.

For bulk calculations, DFT parameters like kinetic cutoff energy value (E_{cut}), k-points set and smearing function, were optimized. This task was carried out using the Methfessel–Paxton first order smearing approach, for the partial occupations of the electronic states near the Fermi level. For all calculations, we used a smearing width of 0.01 eV. Analysis of the system energy shows that the use of a $8 \times 8 \times 8$ gamma centered k-point grid to sample the Brillouin zone and $E_{cut} = 700$ eV, is enough for the total energy to converge to within 10 meV. Geometry optimizations were obtained by minimizing the total energy of the unit cell using a conjugated gradient algorithm to relax ions [28].

Slab models were employed for surface calculations. Surface energy was calculated for slabs with increasing number of layers in order to determine the number of layers necessary for our model. During calculations, DFT parameters previously obtained from bulk optimization and an $8 \times 8 \times 1$ k-points grid were used, concluding that three layers are enough to ensure surface energy convergence (see Table 1). Ooi et al. [29] calculated the surface energy of a graphite (0 0 0 1) surface for a slab with increasing number of layers. They employed the LDA approximation because the GGA approximation without the dispersion contribution fails to generate interplanar bonding. They found oscillating values in 0.075–0.085 J/m^2 range. These oscillations increase with the slab thickness, attributing this behavior to the inability of LDA to reproduce Van der Waals bonding. In our case the inclusion of the Van der Waals term to GGA made the surface energy converge with only a few layers. Eq. (1) was used for calculating the surface energy (σ), where E_{slab} is the total energy of the slab, n_c is the number of carbon atoms of the slab model, A is the surface area, and E_{bulk} is the energy per atom for bulk graphite.

$$\sigma = \frac{E_{slab} - n_c E_{bulk}}{2A} \quad (1)$$

Details on the slab model will be given in the following sections.

Eq. (2) was used to calculate the adsorption energy (E_{ads}), where $E_{Ag_n/surf}$ is the energy of the graphite surface (with or without defects) with n Ag atom adsorbed, where $n = 1$, 2, 3 and 4, E_{surf} is the energy of the clean graphite surface (with or without defects) and E_{Ag} is the energy of an isolated Ag atom.

$$E_{ads} = E_{Ag_n/surf} - E_{surf} - nE_{Ag} \quad (2)$$

With this definition a negative adsorption energy corresponds to a stable adsorption on the surface.

To evaluate the stability of growing Ag nanowires on the step, we define the nanowire formation energy, E_{nw}, as

$$E_{nw} = [E_{(Ag_n/Step)} + E_{(Surface)}] - [E_{(Ag_{n-1}/Step)} + E_{(Ag_1/Terrace)}] \quad (3)$$

E_{nw} determines how easily an Ag_n nanowire is formed on the step from an Ag_{n-1} nanowire on the step and an Ag monomer adsorbed on the terrace. A negative value of this energy indicates a favorable tendency to the formation of a nanowire.

In order to analyze the electronic structure, the electronic charges on atoms were computed using Bader analysis [30] and the atom projected density of states (PDOS) was obtained by projection of the one-electron wave functions onto atomic Bader volumes.

3. Results

3.1. Bulk

In order to test the reliability of our calculations some properties were calculated and compared with experimental data from literature.

A geometry optimization was performed to determine lattice parameters of the graphite hexagonal crystal structure. The unit cell employed is shown in Fig. 1(a). Ion positions, cell volume and cell shape were allowed to simultaneously relax. The calculated lattice parameters are $a = 2.462$ Å and $c = 6.353$ Å. The parameter c is underestimated 5% respect to the experimental value ($a = 2.462$ Å, $c = 6.707$ Å) [31].

The calculated value for the bulk modulus, B, is 34.2 GPa which is in good agreement with experimental data [31–36]. B, was calculated by fitting the energies from a series of constant volume relaxations (i.e., all degrees of freedom except volume have been optimized) to the Birch–Murnaghan equation of state [37,38].

3.2. Clean surface without defects and with a step

The surface was modeled with a slab consisting of three carbon layers within a 4×4 unit cell and a vacuum spacing between slabs of about 22 Å, for the surface without defects (Fig. 1(b)). The size of the supercell is large enough to allow further study of the adsorbed species and the vacuum spacing ensures no interaction between slabs. Being a considerably large supercell, a $3 \times 3 \times 1$ gamma centered k-point-set was used, in this case. For the study of adsorption of more than 3 Ag atoms a larger supercell was employed.

Carbon atoms on the surface were allowed to relax in all directions for the top two layers, keeping the bottom layer fixed. No change in the positions of carbon atoms in the direction parallel to the surface was found, but only in the direction perpendicular to the surface, with an increase in the distance between layers of approximately 0.06 Å. The surface energy calculated was 0.20 J/m^2 which agrees with values reported in literature [39–41]. No magnetization of the surface was observed.

We also studied a stepped surface with the step in the [0 1 0 0] direction. To model the step, some atoms from the top layer of the slab were removed. Fig. 2 shows the 5×4 unit cell slab, used to model the stepped surface. The surface was allowed to relax, keeping the bottom layer fixed. No major change in the C—C bond distance between pairs of carbon atoms on the step was observed, compared to pairs of carbon atoms on the terrace. Spin calculations showed a significant value of the magnetic moment; it is believed that this is due to the decrease in the coordination of carbon atoms forming the step.

3.3. Ag on the surface without defects

The adsorption of Ag on the graphite surface without defects was studied. An Ag atom was placed at specific sites on the surface, and a geometry optimization was performed, allowing the system to relax in order to find the most stable position for Ag on the surface. Fig. 3 shows the different adsorption sites on the graphite surface studied labeled α and β (top sites), H (hollow site) and B (bridge

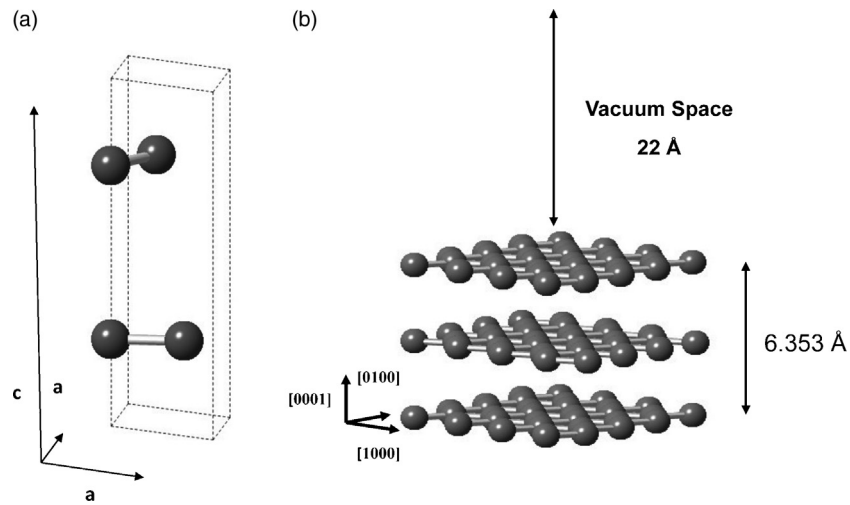

Fig. 1. (a) Bulk graphite unit cell. (b) Slab model constructed with three layers within 4 × 4 unit cells and a vacuum spacing of 22 Å.

site). Top α sites (red circles), Top β sites (gray circles) correspond, respectively, to positions on top of C atoms on the surface, with and without C atoms on the plane below (represented by black circles).

The adsorption energy calculated on each site studied, is negative indicating adsorption is possible on every site. On the bridge site, adsorption is slightly more favorable although there are not large differences between the adsorption energies on top sites. Table 2 summarizes the adsorption energies, magnetic data and geometric parameters calculated for Ag adsorbed on different sites.

Top β site has been previously reported to be the most stable adsorption site after DFT calculations for fixed and relaxed graphite surfaces using LDA functionals [11,12]. This site is believed to be more stable due to the fact that carbon atoms are not bonded to another carbon atom belonging to the plane below, so that π orbitals are free to overlap with the Ag atom orbitals. In order to compare these results with ours, we repeated our calculations fixing the surface without considering the contribution of the dispersion energy, added to the calculations by the DFT-D2 Grimme correction. In this case, Top β site was found to be the most favorable site for Ag, but no stable adsorption energy was found, meaning that no binding occurred when Van der Waals forces are not considered. We also computed the adsorption energies including the dispersion energy, but keeping the surface fixed, and Top-α site was obtained as the most stable site. Hence, the use of a Van der Waals correction method, which properly predicts the forces between graphite layers, influences the adsorption energy calculations. In any case, the difference in the adsorption energies values is small, being within the range of experimental error.

Amft et al. [13] have studied the adsorption of Ag atoms on clean graphene accounting for Van der Waals interactions by both PBE-D2 and vdw-DF methods. They observed that the DFT-D2 method of Grimme overestimates the adsorption energy of Ag on graphene by around 0.5 eV, compared to the vdw-DF method. Granatier et al. [14] also calculated adsorption energies for Ag on a clean graphene sheet by the vdw-DF [42] method obtaining, for the adsorption energy, values of around 0.2 eV, similar to those obtained by Amft et al. [13].

In our work, PBE-D2 and vdw-DF2 methods were employed to calculate Ag adsorption energies on a three layers graphite surface without defects. In this case, the difference in the calculated

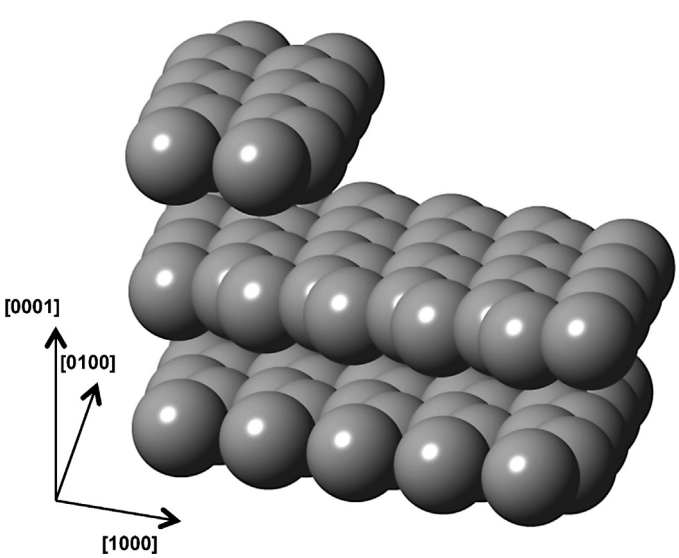

Fig. 2. Graphite surface with a step in the [0 1 0 0] direction, consisting of 5 × 4 unit cells with some top layer atoms removed.

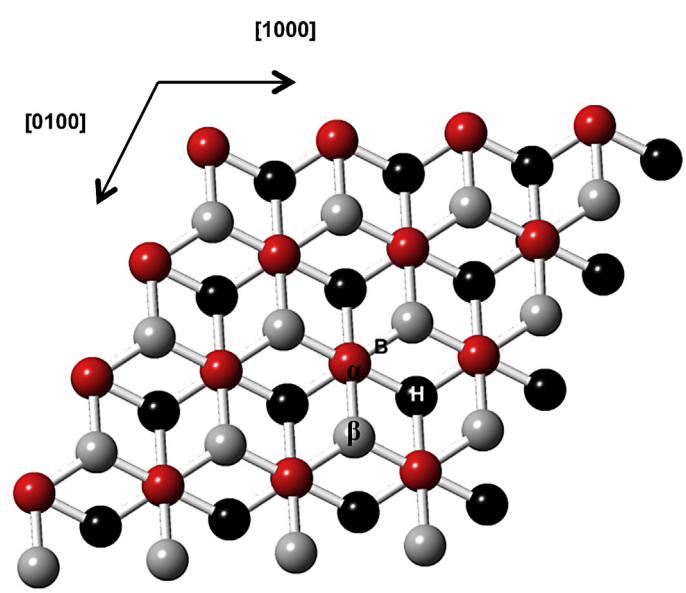

Fig. 3. A top view of the graphite surface, where the black circles represent atoms belonging to the layer below and the red and gray circles represent atoms on the top layer. Sites Top α, Top β, bridge (B) and hollow (H) are indicated. (For interpretation of the references to color in this figure legend, the reader is referred to the web version of this article.)

Table 2
Adsorption energy (E_{ads}), adsorption energy associated to Van der Waals forces ($E_{ads\text{-}vdw}$), magnetic data and geometry parameters associated with the Ag adsorption on the graphite surface without defects, calculated with PBE-D2. The magnitude $d_{Ag\text{-}surf}$ represents the perpendicular distance from Ag to the surface.

Site	E_{ads} (eV)	$E_{ads\text{-}vdw}$ (eV)	Mag. (μ_B)	$d_{Ag\text{-}C\ 1^\circ\ neighbor}$ (Å)	$d_{Ag\text{-}C\ 2^\circ\ neighbor}$ (Å)	$d_{Ag\text{-}surf}$ (Å)
Top-α	−0.30	−0.48	1.10	2.469	2.884	2.487
Top-β	−0.30	−0.49	1.01	2.474	2.877	2.474
Hollow	−0.29	−0.48	1.07	3.064	3.064	2.671
Bridge	−0.32	−0.49	0.97	2.582	2.592	2.493

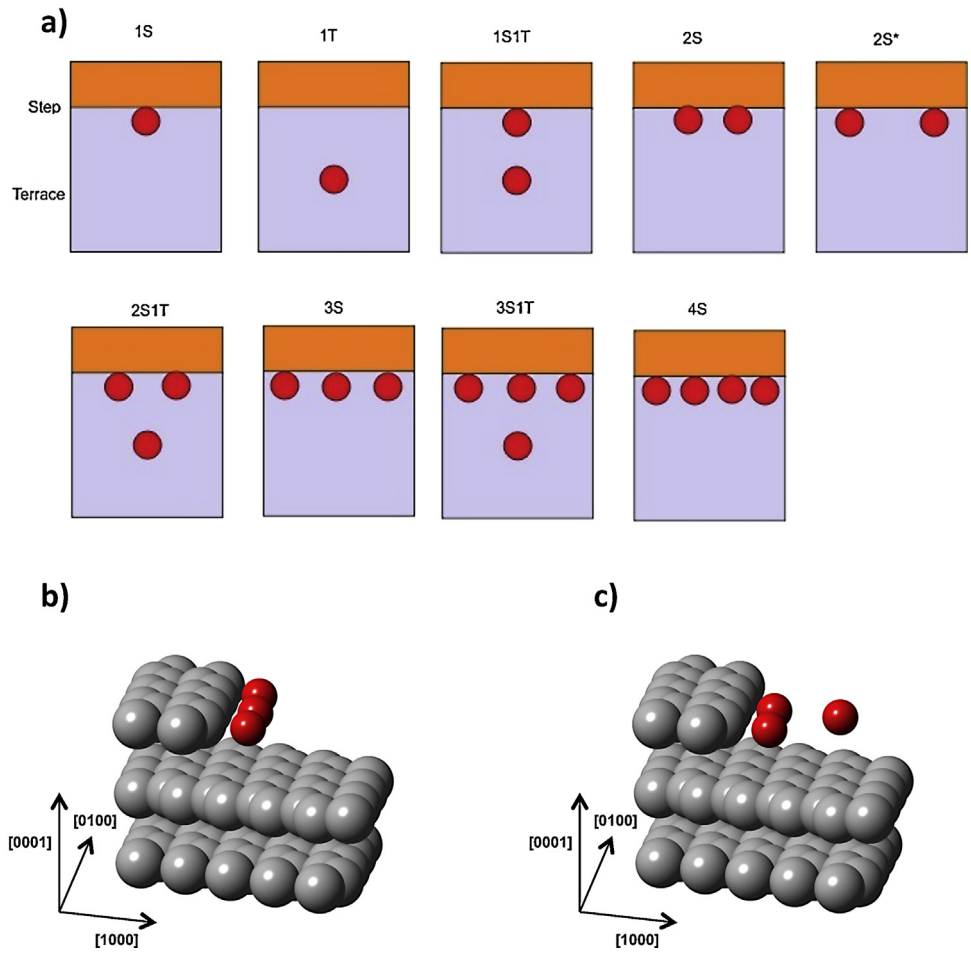

Fig. 4. (a) Schematic representation of the different systems. (b) A three atom Ag nanowire on the step (3S). (c) Structure of two Ag adtoms on the step and another Ag on the terrace (2S1T).

adsorption energy values by both methods, is 0.1 eV. If we look at the contribution to the adsorption energy of the Van der Waals forces ($E_{ads\text{-}vdw}$) in Table 2, it can be seen that the stabilization of the system is dominated by the dispersion forces. This conclusion was also obtained by other authors, which found no bond between the Ag and graphene surface without the contribution of Van der Waals forces [13–15]. We believe that the better agreement between the values of the adsorption energy calculated with both methods on graphite surface compared to the greater difference on graphene; is due to the Coulombic repulsion arising between the Ag and the C atoms on the graphite surface which compensates for the attractive semiempirical energy term of the model proposed by Grimme [26] to account the Van der Waals forces. The values of the adsorption energies for Ag on graphite calculated by the vdw-DF2 method are shown in Table 3. We can observe in these results a closer match with adsorption energies calculated for Ag adatom on graphene [13–15]. The predictions are also very similar to that reported by Singh et al. [16] for graphite.

3.4. Ag on the stepped surface

In order to explore the deposition of Ag on a stepped graphite surface, different systems consisting of the stepped surface with increasing amounts of adsorbed Ag atoms with various geometric configurations were studied. In a first stage, two possible adsorption sites for the first Ag adatom were considered: on a terrace and in the vicinity of the step. It was found that

Table 3
Adsorption energy (E_{ads}) and magnetic data associated with the Ag adsorption on the graphite surface without defects, calculated with vdw-DF2.

Site	E_{ads} (eV)	Mag. (μ_B)
Top-α	−0.21	1.00
Top-β	−0.24	1.01
Hollow	−0.20	0.98
Bridge	−0.23	1.00

Table 4
Adsorption energy (E_{ads}), adsorption energy associated to Van der Waals forces ($E_{ads\text{-}vdw}$), nanowire formation energy (E_{nw}), magnetic data and geometry parameters associated with the Ag adsorption on the graphite surface with step in the [0 1 0 0] direction, calculated with PBE-D2.

System	E_{ads} (eV)	$E_{ads\text{-}vdw}$ (eV)	E_{nw} (eV)	Mag. (μ_B)	$d_{Ag\text{-}C,\ 1^\circ\ neighbor\ on\ terrace}$ (Å)	$d_{Ag\text{-}C,\ 1^\circ\ neighbor\ on\ step}$ (Å)	$d_{Ag\text{-}Ag}$ (Å)
1S	−3.05	−0.54	–	5.14	2.871	2.106	–
1T	−2.75	−0.54		4.85	2.698	–	–
2S*	−6.24	−1.07	–	4.45	2.970	2.104	4.922
2S	−6.49	−1.03	−0.70	4.45	3.064	2.113	2.855
1S1T	−5.91	−0.95	–	4.44	3.275	1.902	2.485
3S	−10.01	−1.67	−0.77	5.00	3.113	2.123	3.198
2S1T	−8.82	−1.59	–	3.07	3.150	2.124	3.657
4S	−12.41	−2.10	−0.99	4.45	2.687	2.166	2.702
3S1T	−10.37	−2.00	–	5.53	3.156	2.173	3.463

the most favorable site was on the step with an adsorption energy of −3.05 eV almost 0.3 eV more stable than adsorption on the terrace (−2.75 eV). This behavior is due to the fact that the Ag atom can interact with more carbon atoms on the step.

For the system with one Ag on the step, another Ag atom was added. Three different adsorption sites were considered, on the terrace, on the step next to the first Ag atom and on the step separate from the first Ag atom. In this case, the Ag atom prefers to adsorb, next to the other Ag atom on the step.

Consecutively the other systems were built following the same procedure. Keeping the most stable configuration and looking for the most favorable adsorption sites for an extra Ag atom, always considering the possibility of adsorption on the terrace and on the step. The process was continued until a system consisting of four Ag atoms on the surface was built. To describe these systems the following nomenclature is used. A number followed by the letter S, indicates the number of Ag atoms on the step, a number followed by the letter T, indicates the number of Ag atoms on the terrace. The case 2S* represents a system consisting of two Ag atoms on the step but apart from each other, in order to evaluate the tendency of Ag atoms on the step to interact with each other. Fig. 4(a), shows a schematic representation all the systems previously described, (b) and (c) shows the systems 3S and 2S1T respectively. Table 4 summarizes energy data and geometry parameters for the different systems studied.

The adsorption energy for the system 1S is more negative than for the system 1T, indicating a preference for Ag atom to locate on the step. This behavior is repeated in systems with two, three and four atoms, suggesting the preference of Ag atoms to adsorb on the step instead of on the terrace, resulting in the formation of Ag nanowires on the steps of graphite. In particular, for the case of two Ag atoms adsorbed on the step, 2S is more stable than 2S*, another indication that when the atoms locate on the step, they prefer to remain close together minimizing the total energy by interacting with each other.

Table 5
Adsorption energy (E_{ads}), nanowire formation energy (E_{nw}), associated with the Ag adsorption on the graphite surface with step in the [0 1 0 0] direction, calculated with vdw-DF2.

System	E_{ads} (eV)	E_{nw} (eV)
1S	−2.60	–
1T	−2.45	–
2S*	−5.18	–
2S	−5.30	−0.25
1S1T	−4.85	–

In order to verify this tendency, we calculated the nanowires formation energy for two Ag atoms on the stepped surface, using the vdw-DF2 method. The calculated adsorption and nanowires formation energies are shown in Table 5. We observe that PBE-D2 method gives higher values for the adsorption energies than the vdw-DF2 method. But in terms of relative differences, (i.e., E_{ads} calculated with PBE-D2 minus E_{ads} calculated with vdw-DF2 divided E_{ads} calculated with vdw-DF2), the difference on the stepped surface decreases considerably with respect to the calculations performed on the surface without defects. For the surface without defects the relative difference was closely 50% while for the surface with a step, it was around 20%. This decrease can be understood if we look at the adsorption energies corresponding to dispersion forces in Table 4. This energy is only a fraction less than 0.2 of the total energy of adsorption meaning that the nature of the binding in the case of a stepped surface with Ag adatoms is more chemical than physical. In this case the overestimation made by PBE-D2 method for this physical interaction does not affect in the same way. So, despite the difference in the calculated energy, both methods predict the possibility of nanowire formation, although the driving force predicted by the PBE-D2 method is larger.

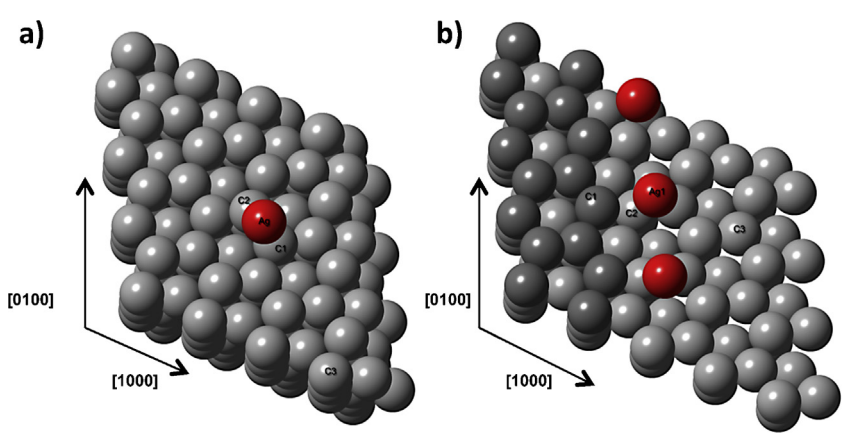

Fig. 5. (a) Graphite surface without defects with an Ag adatom on bridge site and (b) three Ag nanowire on the stepped graphite surface. Ag and C atoms taken as reference for charge calculations are labeled.

Table 6
Net charges for selected atoms when an Ag atom is adsorbed on different sites on the (0 0 0 1) graphite surface.

Site	C1	C2	C3	Ag
Clean surface	0.100	−0.097	0.100	–
Bridge	−0.085	−0.189	0.106	0.218
Top-α	−0.077	−0.149	0.102	0.217
Hollow	−0.087	0.074	−0.086	0.143

Table 7
Net charges for selected atoms when an Ag atom is adsorbed on (0 0 0 1) graphite surface with a step in the [0 1 0 0] direction.

System	C1	C2	C3	Ag	Ag on terrace
Clean surface	−0.087	−0.010	0.026	–	–
1T	−0.026	−0.086	0.067	–	0.444
1S	−0.106	−0.124	−0.081	0.425	–
2S	−0.112	−0.120	0.021	0.345	–
2S*	−0.087	−0.106	0.020	0.407	–
1S1T	−0.117	−0.117	0.019	0.361	0.344
3S	−0.112	−0.110	0.018	0.314	–
2S1T	−0.104	−0.015	0.004	0.362	0.236
4S	−0.123	−0.054	−0.088	0.288	–
3S1T	−0.111	−0.111	−0.001	0.258	0.272

The interaction between Ag atoms was also investigated calculating the binding energy on an isolated dimmer. For the calculation, a cell of 10 × 10 × 10 Å and a k-mesh formed by Γ point only was used. The results gave a binding energy of −1.76 eV for PBE-D2 method with a equilibrium bond length, r_{Ag-Ag} = 2.59 Å, and in the case vdw-DF2 method we obtained −1.74 eV and r_{Ag-Ag} = 2.65 Å. Based on these values, both methods gave similar results to quantified Ag–Ag interaction and are in good agreement with the experimental value of −1.65 eV [43] and r_{Ag-Ag} = 2.53 Å [44]. So the main difference between both methods for the estimation of the energies of formation of nanowires comes from the C–Ag interaction.

The negative formation energy for each nanowire, indicates an energy gain when the Ag_n nanowire is formed on the surface step compared to the Ag_{n-1} nanowire on the step and an single Ag atom adsorbed on the terrace. So, since adsorption is possible on either the step or the terrace, as can be seen by the negative adsorption energies in Table 4, it is possible for Ag atoms to adsorb on the terraces and then diffuse superficially to the steps where they reach the most stable configuration.

Ag—C bond distance is shorter when C adsorbs on the step than when it locates on terraces, suggesting greater interaction between Ag and the C atoms on the steps. This stronger bond between them leads to more stability. The average bond distance between Ag atoms, is also shorter when the atoms locate on the step.

3.5. Electronic structure analysis

Bader analysis was employed to determine the charge densities for the different systems. In all cases a charge transfer from the Ag adatoms to C atoms on the surface is observed. The amount of charge transferred is larger when the Ag atom adsorbs on the step (∼0.4 e⁻) than when it when it adsorbs on the surface without defects (∼0.2 e⁻). Table 6 shows the computed charges on selected atoms for the surface without defects before and after Ag adsorption on different sites. C1 and C2 indicate carbon atoms first neighbors to Ag, and C3 is a carbon atom distant from the Ag atom. C1 and C3 are β-type carbons while C2 is an α-type carbon. For the clean surface C1 and C3 are slightly positive, while C2 is negative probably due to the interaction with the carbon atom on the plane below. When Ag atom adsorbs on the surface, in every case, there is a charge transfer from Ag to its closest neighbors C1 and C2. The largest transfer occurs to C2, which increases its charge about 0.18 e⁻. Fig. 5(a) shows the Ag atom adsorbed on a bridge site on the surface without defects as well as C1, C2 and C3. Since the adsorption energies calculated in previous section are not negative without the term of dispersive forces this transfer is not enough to unscreen the repulsion of nucleus and occurs only because of the proximity of the adatoms to the surface. This is consistent with the fact that the sites with larger charge transference are those with the Ag adatom nearer to the surface (see Tables 2 and 6). For the stepped surface Table 7 shows the charges calculated for each

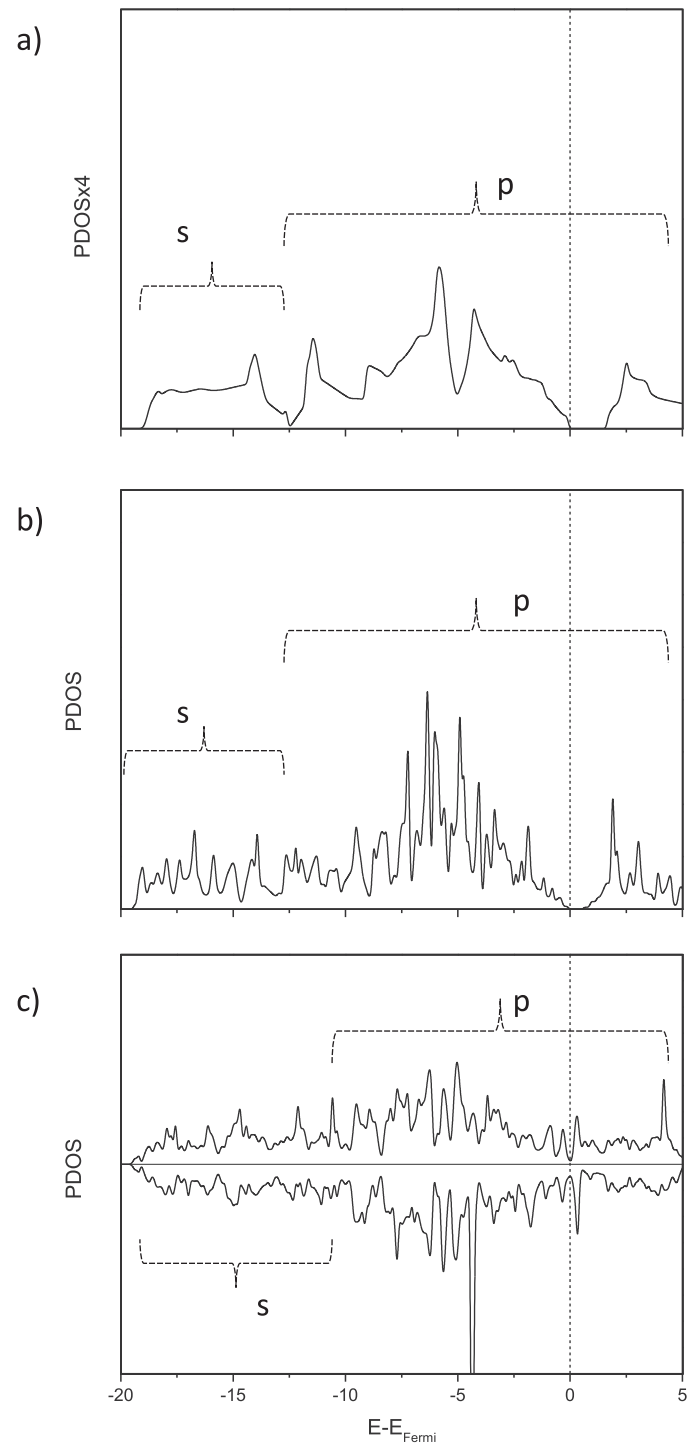

Fig. 6. (a) Total density of states for bulk graphite, (b) PDOS on surface atoms for the clean (0 0 0 1) surface without defect and (c) PDOS on surface atoms for the clean (0 0 0 1) surface with a step in the [0 1 0 0].

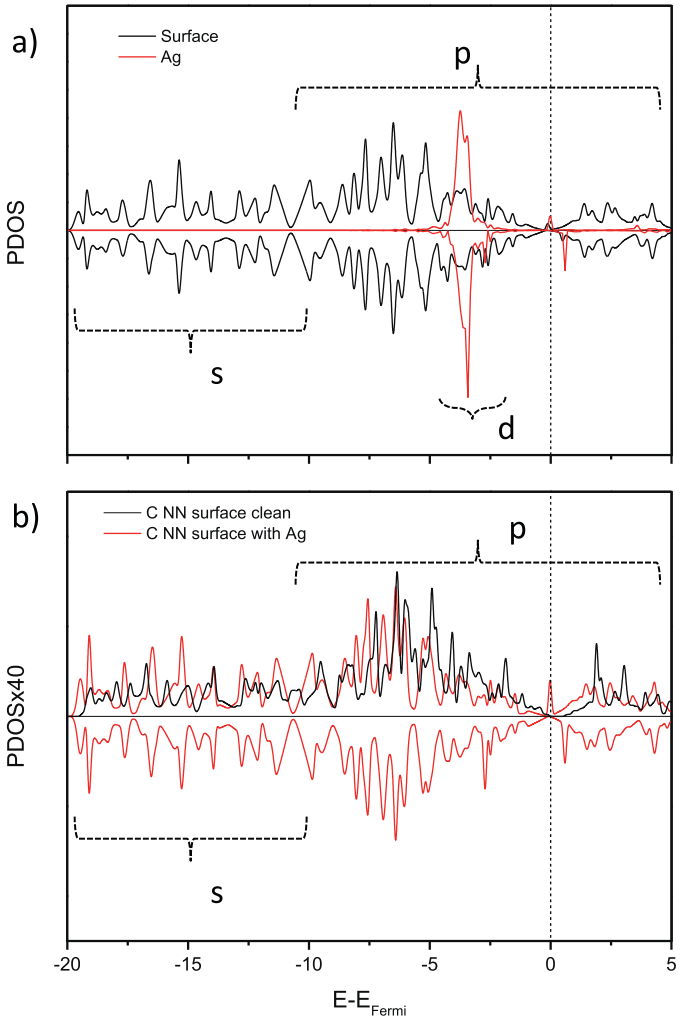

Fig. 7. PDOS on the (a) surface atoms for the surface without defect with an Ag adatom, (b) C NN atom on the surface without defects, before and after the Ag atom adsorption.

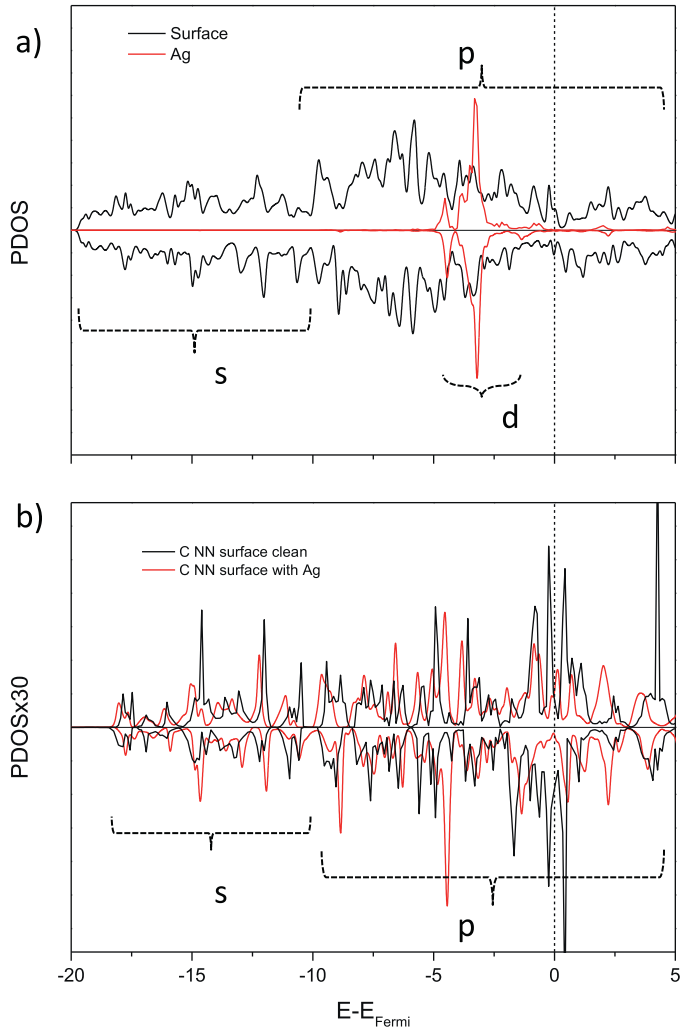

Fig. 8. PDOS on (a) the surface atoms for the stepped surface with an Ag adatom, (b) a C NN atom on the stepped surface before and after the Ag atom adsorption.

system studied. In this case, C1 and C2 indicate carbon atoms first neighbors to Ag on the step and on the terrace, respectively, and C3 is a carbon atom distant from Ag (see Fig. 5(b)). The Ag adatom is also positively charged when it is adsorbed on the surface with a step, with larger electron transference than for the surface without defects. For different systems studied, the Ag atom loses from 0.26 to 0.44 e^- toward its C neighbors.

Total density of state for bulk graphite and PDOS curves on surface atoms for clean surface with and without defects are shown in Fig. 6. Peaks corresponding to the s orbital are observed in the lower range of energy with respect to E_f, between −20 and −10 eV, while the p orbitals locate at higher energies, between −10 and 13 eV. There is a small band gap of about, 1.3 eV, for bulk graphite, which is smaller for the surface without step, and disappears for the surface with step, as can be seen in Fig. 6(c).

For Ag adsorbed on the surface without defects, PDOS on surface atoms is presented in Fig. 7(a). A peak corresponding to Ag d states is observed at about −3.5 eV, which interact with C p orbitals inside the valence band. Fig. 7(b) shows the PDOS on a C atom nearest neighbor (NN) to Ag before and after Ag adsorption. Occupied states shift to lower energies and the difference in the spin up and down contributions to the PDOS, below E_f, accounts for the increase in the magnetic moment.

Fig. 8 shows PDOS on surface atoms and on a C atom nearest neighbor to Ag for the stepped surface. In this case a broader region, around 4.5 eV, corresponds to Ag d orbitals, resulting in a stronger interaction between Ag and C atoms of the graphite.

4. Conclusions

Adsorption of Ag atoms on graphite surface with and without defects was studied by DFT calculations. A bridge site was found to be the most favorable site for Ag adsorption on the surface without defects, although other sites are also stable. The value of the calculated adsorption energies changes when the Van der Waals effect is not considered, and no bond is observed in this case. The adsorption energy increases considerably when the adsorption occurs on stepped surfaces. In this case, the Ag adatoms prefer to locate on the step instead of on the terrace. In addition, when the atoms locate on the step, they prefer to remain close to each other, making possible the formation of nanowires structures of different lengths, depending of the magnitude of the step. In addition, the adsorption of increasing amounts of Ag on the step lead to more stable structures. A charge transfer from Ag atoms to carbon atoms on the surface is observed. The transfer is larger for the stepped surface where Ag adatoms become positively charged and the major e^- transference occurs toward the C atom below the Ag adatom instead to the C atom on the step. PDOS analysis shows an increase of occupied states corresponding to Ag d orbitals for the case of Ag adsorbed on the step, giving a more stable structure.

Acknowledgments

The authors are grateful for the financial support from PICT 1770, SGCyT-UNS PGI 24/F048 and PGI24/F128. R. E. Ambrusi and M. E. Pronsato are members of CONICET.

References

[1] B. Bhushan (Ed.), Handbook of Nanotechnology, 2nd ed., Springer, Berlin, 2007.
[2] R. Penner, in: R.E. White (Ed.), Modern Aspects of Electrochemistry, vol. 45, Springer, Irvine, 2009, pp. 175–206.
[3] B.J. Murray, E.C. Walter, R.M. Penner, Amine vapor sensing with silver mesowires, American Chemical Society, Nanoletters 4 (2004) 665–670.
[4] C. Bréchignac, Ph. Cahuzac, F. Carlier, C. Colliex, J. Leroux, A. Masson, B. Yoon, U. Landman, Inestability driven fragmentation of nanoscale fractal islands, Phys. Rev. Lett. 88 (2002) 196103-1–196303-2.
[5] S.J. Carroll, S. Pratontep, M. Streun, R.E. Palmer, S. Hobday, R.J. Smith, Pinning of size-selected Ag clusters on graphite surfaces, Chem. Phys. 113 (2000) 7723–7727.
[6] W. Yamaguchi, K. Yoshimura, Y. Tai, Y. Maruyama, K. Igarashi, S. Tanemura, J. Murakami, Energy-dependent deposition processes of size-selected Ag nanoclusters on highly-oriented pyrolytic graphite, J. Chem. Phys. 112 (2000) 9961–9966.
[7] D.J. Kenny, R.E. Palmer, C.F. Sanz-Navarro, R. Smith, Implantation depth of size-selected silver clusters into graphite, J. Phys.: Condens. Matter 14 (2002) L185–L191.
[8] N.R. Gall, E.V. Rut'kov, A.Ya. Tontegode, Anomalous behavior of silver atoms in intercalation under a two-dimensional graphite film, JETP Lett. 75 (2002) 26–28.
[9] A. Courty, I. Lisiecki, M.P. Pileni, Vibration of self-organized silver nanocrystals, J. Chem. Phys. 116 (2002) 8074–8078.
[10] G.F. Ndlovu, D.W. Roos, Z.M. Wang, J. Asante, M.G. Mashapa, C.J. Jafta, B.W. Mwakikunga, K.T. Hillie, Epitaxial deposition of silver ultra-fine nano-clusters on defect-free surfaces of HOPG-derived few-layer graphene in a UHV multi-chamber by in situ STM, ex situ XPS, and ab initio calculations, Nanoscale Res. Lett. 7 (1) (2012) 173.
[11] D.M. Duffy, J.A. Blackman, The energy of Ag adatoms and dimers on graphite, Surf. Sci. 415 (1998) L1016–L1019.
[12] G.M. Wang, J.J. DelBruno, S.D. Kenny, R. Smith, Interaction of silver adatoms and dimers with graphite surfaces, Surf. Sci. 541 (2003) 91–100.
[13] M. Amft, S. Lebègue, O. Eriksson, N.V. Skorodumova, Adsorption of Cu, Ag, and Au atoms on graphene including van der Waals interactions, J. Phys.: Condens. Matter 23 (2011) 395001.
[14] J. Granatier, P. Lazar, M. Otyepka, P. Hobza, The nature of the binding of Au, Ag, and Pd to benzene, coronene, and graphene: from benchmark CCSD(T) calculations to plane-wave DFT calculations, J. Chem. Theory Comput. 7 (2011) 3743–3755.
[15] J.-P. Jalkanen, M. Halonen, D. Fernández-Torre, K. Laasonen, L. Halonen, A Computational study of the adsorption of small Ag and Au nanoclusters on graphite, J. Phys. Chem. A 111 (2007) 12317.
[16] A. Singh, C. Majumder, P. Sen, Do Ag_n (up to $n = 8$) clusters retain their identity on graphite? Insights from first-principles calculations including dispersion interactions, J. Chem. Phys. 140 (2014) 164705.
[17] E. Ganz, K. Sattler, J. Clarke, Scanning tunneling microscopy of the local atomic structure of two-dimensional gold and silver islands on graphite, Phys. Rev. Lett. 60 (1988) 1856–1859.
[18] E. Ganz, K. Sattler, J. Clarke, Scanning tunneling microscopy of Cu, Ag, Au and Al adatoms, small clusters, and islands on graphite, Surf. Sci. 219 (1989) 33–67.
[19] G. Kresse, J. Hafner, Ab initio molecular dynamics for open-shell transition metals, Phys. Rev. B 48 (1993) 13115–13118.
[20] G. Kresse, J. Hafner, Ab initio molecular-dynamics simulation of the liquid–metal–amorphous-semiconductor transition in germanium, Phys. Rev. B 49 (1994) 14251–14269.
[21] G. Kresse, J. Furthmv̈ller, Efficiency of ab-initio total energy calculations for metals and semiconductors using a plane-wave basis set, Comput. Mater. Sci. 6 (1996) 15–50.
[22] G. Kresse, J. Furthmv̈ller, Efficient iterative schemes for ab initio total-energy calculations using a plane-wave basis set, Phys. Rev. B 54 (1996) 11169–11186.
[23] J.P. Perdew, K. Burke, M. Ernzerhof, Generalized gradient approximation made simple, Phys. Rev. Lett. 77 (1996) 3865–3868.
[24] P.E. Blöchl, Projector augmented-wave method, Phys. Rev. B 50 (1994) 17953–17979.
[25] G. Kresse, D. Joubert, From ultrasoft pseudopotentials to the projector augmented-wave method, Phys. Rev. B 59 (1999) 1758–1775.
[26] S. Grimme, Semiempirical GGA-type density functional constructed with long-range dispersion correction, J. Comp. Chem. 27 (2006) 1787–1799.
[27] J. Klimeš, D.R. Bowler, A. Michaelides, Chemical accuracy for the van der Waals density functional, J. Phys.: Condens. Matter 22 (2010) 022201.
[28] W.H. Press, B.P. Flannery, S.A. Teukolsky, W.T. Vetterling, Numerical Recipies, Cambridge University Press, New York, 1986.
[29] N. Ooi, A. Rairkar, J.B. Adams, Density Functional study of graphite bulk and surface properties, Carbon 44 (2006) 231–242.
[30] R.F.W. Bader, Atoms in Molecules – A Quantum Theory, Oxford University Press, Oxford, 1990.
[31] O.A. Von Lilienfeld, A. Tkatchenko, Two- and three-body interatomic dispersion energy contributions to binding in molecules and solids, J. Chem. Phys. 132 (2010) 234109.
[32] P. Jinwoo, D.Y. Byung, H. Suklyun, Ab initio calculations with van der Waals corrections: benzene–benzene intermolecular case and graphite, J. Korean Phys. Soc. 59 (2011) 196–199.
[33] Y.X. Zhao, I.L. Spain, X-ray diffraction data for graphite to 20 GPa, Phys. Rev. B 40 (1989) 993–997.
[34] R.C.E. Weast, CRC Handbook of Chemistry and Physics, 65th ed., CRC Press, Boca Raton, FL, 1984–1985, pp. D58.
[35] M. Hanfland, H. Beister, K. Syassen, Graphite under pressure: equation of state and first-order Raman modes, Phys. Rev. B 39 (1989) 12598–12603.
[36] T. Bučko, J. Hafner, S. Lebegue, J.G. Angyán, improved description of the structure of molecular and layered crystals: ab initio DFT calculations with van der Waals corrections, J. Phys. Chem. A 114 (2010) 11814–11824.
[37] F. Birch, The Effect of pressure upon the elastic parameters of isotropic solids, according to Murnaghan's theory of finite strain, J. Appl. Phys. 9 (1938) 279–288.
[38] F. Birch, Finite elastic strain of cubic crystals, Phys. Rev. 71 (1947) 809–824.
[39] N. Eustathopoulos, M.G. Nicholas, B. Drevet, Pergamon Materials Series: Wettability at High Temperatures, Elsevier Science, Amsterdam, 1999.
[40] H. Zaidi, F. Robert, D. Paulmier, Influence of adsorbed gases on the surface energy of graphite: consequences on the friction behavior, Thin Solid Films 264 (1995) 46–51.
[41] J. Abrahamson, The surface energies of graphite, Carbon 11 (1975) 337–362.
[42] M. Dion, H. Rydberg, E. Schröder, D.C. Langreth, B.I. Lundqvist, Van der Waals density functional for general geometries, Phys. Rev. Lett. 95 (2005) 109902.
[43] M.D. Morse, Clusters of transition-metal atoms, Chem. Rev. 86 (1986) 1049.
[44] B. Simard, P.A. Hackett, A.M. James, P.R.R. Langridge-Smith, The bond length of silver dimer, Chem. Phys. Lett. 186 (1991) 415.